Near-Earth initiation of a terrestrial substorm

Near-Earth initiation of a terrestrial substorm

I. Jonathan Rae,[1] Ian R. Mann,[1] Vassilis Angelopoulos,[2] Kyle R. Murphy,[1] David K. Milling,[1] Andy Kale,[1] Harald U. Frey,[3] Gordon Rostoker,[1] Christopher T. Russell,[2] Clare E. J. Watt,[1] Mark J. Engebretson,[4] Mark B. Moldwin,[5] Stephen B. Mende,[3] Howard J. Singer,[6] and Eric F. Donovan[7]

Received 4 October 2008; revised 13 April 2009; accepted 22 April 2009; published 21 July 2009.

[1] Despite the characterization of the auroral substorm more than 40 years ago, controversy still surrounds the processes triggering substorm onset initiation. That stretching of the Earth's magnetotail following the addition of new nightside magnetic flux from dayside reconnection powers the substorm is well understood; the trigger for explosive energy release at substorm expansion phase onset is not. Using ground-based data sets with unprecedented combined spatial and temporal coverage, we report the discovery of new localized and contemporaneous magnetic wave and small azimuthal scale auroral signature of substorm onset. These local auroral arc undulations and magnetic field signatures rapidly evolve on second time scales for several minutes in advance of the release of the auroral surge. We also present evidence from a conjugate geosynchronous satellite of the concurrent magnetic onset in space as the onset of magnetic pulsations in the ionosphere, to within technique error. Throughout this time period, the more poleward arcs that correspond to the auroral oval which maps to the central plasma sheet remain undisturbed. There is good evidence that flows from the midtail crossing the plasma sheet can generate north-south auroral structures, yet no such auroral forms are seen in this event. Our observations present a severe challenge to the standard hypothesis that magnetic reconnection in stretched magnetotail fields triggers onset, indicating substorm expansion phase initiation occurs on field lines that are close to the Earth, as bounded by observations at geosynchronous orbit and in the conjugate ionosphere.

Citation: Rae, I. J., et al. (2009), Near-Earth initiation of a terrestrial substorm, *J. Geophys. Res.*, *114*, A07220, doi:10.1029/2008JA013771.

1. Introduction

[2] Energy transferred from the solar wind into near-Earth space is stored and released to power aurorae and generate energetic particle populations during the "loading and unloading" cycle [*Baker et al.*, 1985] of magnetic substorms [*Akasofu*, 1964]. Energy is stored in the stretched nightside magnetic fields which occur when magnetic reconnection connects solar wind and terrestrial magnetic fields at the dayside magnetopause during the substorm growth phase [*McPherron*, 1972]. Magnetic energy is explosively released during substorm expansion phase onset [*Akasofu*, 1964; *McPherron*, 1979]; however, the physics and the location of the region initiating the onset of the substorm expansion have remained controversial for decades [e.g., *Lui*, 1991].

[3] Understanding the physical processes leading to magnetic energy release at substorm expansion phase onset has been limited by the inability to temporally and spatially resolve the causal sequence of events leading up to and during the first two minutes of onset [*Lui*, 1991]. There are two models proposed for the initiation of energy release at substorm expansion phase onset. In one model, substorm expansion phase onset is initiated by magnetic reconnection at a near-Earth neutral line [*Hones*, 1976] (NENL) at a distance of $\sim$20–30 R_E [*Nagai et al.*, 1998]; all subsequent disturbances both closer to and further from the Earth follow after the reconnection ("outside-to-in"; C$\rightarrow$A$\rightarrow$ B in Figure 1c). The second model ("inside-to-out") invokes instabilities and current disruption (CD) in the nearer Earth plasma sheet at $\leq$ 12 Re as the initiator of the onset process [*Roux et al.*, 1991; *Lui et al.*, 1991; *Voronkov et al.*, 1997].

[1]Department of Physics, University of Alberta, Edmonton, Alberta, Canada.
[2]Institute of Geophysics and Planetary Physics, University of California, Los Angeles, California, USA.
[3]Space Sciences Laboratory, University of California, Berkeley, California, USA.
[4]Department of Physics, Augsburg College, Minneapolis, Minnesota, USA.
[5]Department of Earth and Space Sciences, University of California, Los Angeles, California, USA.
[6]NOAA Space Environment Center, Boulder, Colorado, USA.
[7]Department of Physics and Astronomy, University of Calgary, Calgary, Alberta, Canada.

0148-0227/09/2008JA013771

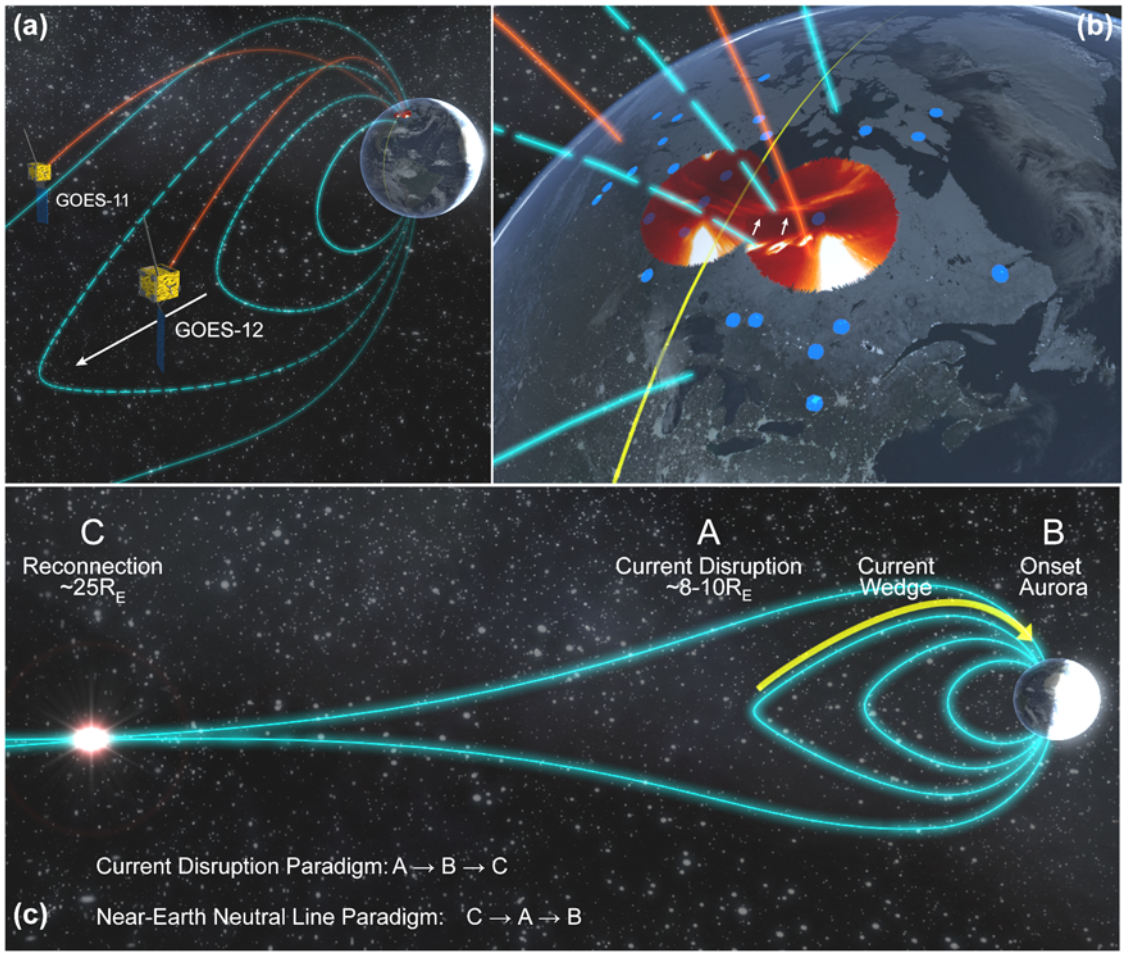

Figure 1. Schematic of the substorm onset paradigm. (a) Locations of GOES 12 (east) and GOES 11 (west) and nominal field lines (red) traced to their T96 [*Tsyganenko*, 1995] ground magnetic footprint (note magnetic substorm magnetic topology means that there are uncertainties in field mapping from GOES to the ground). (b) GILL and SNKQ ASI images from 0553:33 UT, ground magnetometer station locations (blue dots), and midnight geographic meridian (yellow). White arrows indicate the inferred propagation of information, i.e., poleward in the ionosphere, and correspondingly tailward in the magnetosphere. (c) Schematic of the two substorm onset paradigms: "inside-to-out" current disruption [*Roux et al.*, 1991; *Lui et al.*, 1991; *Voronkov et al.*, 2000] (A→B→C) or "outside-to-in" NENL [*Hones*, 1976; *Nagai et al.*, 1998] reconnection (C→A→B). Field lines in Figures 1a–1c are schematic representations but are shown consistently from image to image.

In this latter model, energy is still stored during the growth phase by dayside merging, but is only released in the magnetotail by the process of magnetic reconnection much later in the substorm sequence following the development of near-Earth instabilities and once outward propagating disturbances from this nearer-Earth process reach the NENL (A→B→C current disruption in Figure 1c).

[4] Here we use ground-based all-sky imager and magnetometer data with an unprecedented combination of coverage and temporal resolution to time, locate, and identify a new first indication of substorm expansion phase onset which can be characterized in terms of a combination of magnetic and optical auroral signatures and which we describe here. This new signature indicates isolated substorm initiation characterized by periodic auroral undulations and beads coincident in both time and space with the localized onset of magnetic fluctuations in the Pi1 (1–40 s period) band [*Jacobs et al.*, 1964] at low magnetic latitudes of ~64° (L~5.5). Discrete wavelet analysis shows that magnetic disturbances initiate at, and propagate coherently away from, a longitudinally localized region where an isolated auroral arc begins to evolve on second time scales through an inverse cascade into a series of vortices. That the onset and evolution of the magnetic wave and the auroral features continue for around ~2.5 min prior to the development of the Westward Traveling Surge [*Akasofu et al.*, 1965] strongly support the hypothesis that the substorm begins on field lines that are normally in the dipolar region of the magnetosphere. The new onset signatures reported here very rapidly develop azimuthally periodic auroral arc structure with characteristic time scales of seconds, the development continuing for ~2.5 min in the transition region between taillike and dipolar field lines and a region thought to be unstable to, for example, the growth of both the ballooning mode [e.g., *Roux et al.*, 1991] (see also the review by *Miura* [2001]) and the cross-field current insta-

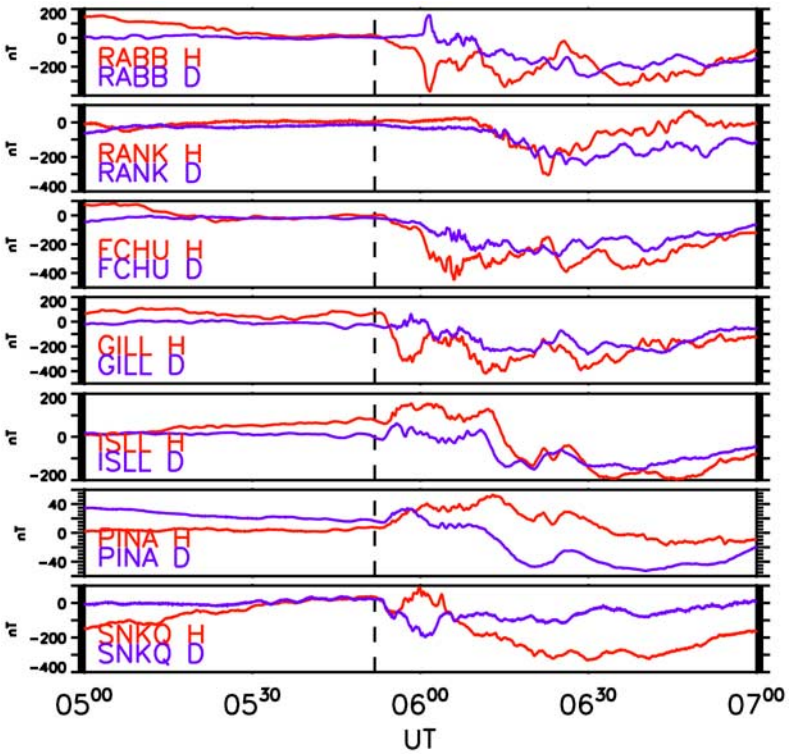

Figure 2. The H and D component magnetograms from selected CARISMA and CANMOS magnetometer stations from 0500 to 0700 UT on 7 March 2007. From top to bottom, Figure 2 shows the stations arranged from west to east and from north to south. The dashed line marks the ULF wave onset at 0551:48 UT.

bility [e.g., *Lui et al.*, 1991]. Throughout this time, the more poleward preexisting discrete arcs which map from the central plasma sheet to the last closed field line at the edge of the polar cap remain undisturbed. As described by *Elphinstone et al.* [1995], the post expansion phase auroral oval often exhibits a so-called ''double-oval'' morphology. In this configuration, activations at the poleward edge such as poleward boundary intensifications (PBIs) [e.g., *Lyons et al.*, 1999] occur independently of activations on the more equatorial branch. We suggest that a similar paradigm may describe the substorm onset process such that activations at the low- and high-latitude auroral oval can be triggered independently. Our observations provide very strong evidence in favor of the importance of near-Earth plasma sheet instabilities as the initiator of expansion phase onset at the equatorial edge of the oval, challenging the standard paradigm that NENL reconnection initiates all substorms.

2. Instrumentation and Methodology

[5] We use high-cadence magnetic measurements from 7 March 2007 from an extensive network of ground-based magnetometers across the North American continent, principally the Canadian Array for Real-time Investigations of Magnetic Activity (CARISMA) (http://www.carisma.ca) [*Mann et al.*, 2008] and Time History and Events and Macroscale Interactions during Substorms (THEMIS) magnetometer arrays [*Sibeck and Angelopoulos*, 2008; *Russell et al.*, 2008] and supported by stations from other networks. The magnetometer measurements and high-cadence 3-s optical measurements from the THEMIS all-sky imager (ASI) array [*Mende et al.*, 2008] are used to study the auroral signatures of substorm expansion phase onset. Figures 1a and 1b show a schematic of the locations of the geosynchronous GOES satellites in the Canadian sector [*Singer et al.*, 1996], the ground-based magnetometers, and false color images from two of the white light ASIs from the THEMIS Ground-based Observatory (GBO) array at Gillam (GILL; L = 6.04) and Sanikiluaq (SNKQ; L = 6.50). Figure 1c shows a schematic highlighting the two different substorm onset paradigms of NENL and CD, where blue lines are schematic representations of magnetic field lines, while red lines represent T96 magnetic field model connectivity between the ground and in situ GOES measurements.

[6] We use the discrete wavelet transform (DWT) technique utilizing Meyer wavelet basis functions detailed by *Murphy et al.* [2009] and *Rae et al.* [2009] to show that the first appearance of disturbances in the Pi1 band can both time and locate the region associated with the first moments of substorm expansion phase onset initiation in the ionosphere. Combined with optical measurements from the THEMIS ASIs, we reveal for the first time a clear sequence of the rapid evolution of new equatorward magnetic and auroral arc activity during the first tens of seconds following onset.

3. Results

[7] Figure 2 shows the H and D component magnetograms from selected magnetometer stations from 0500 to

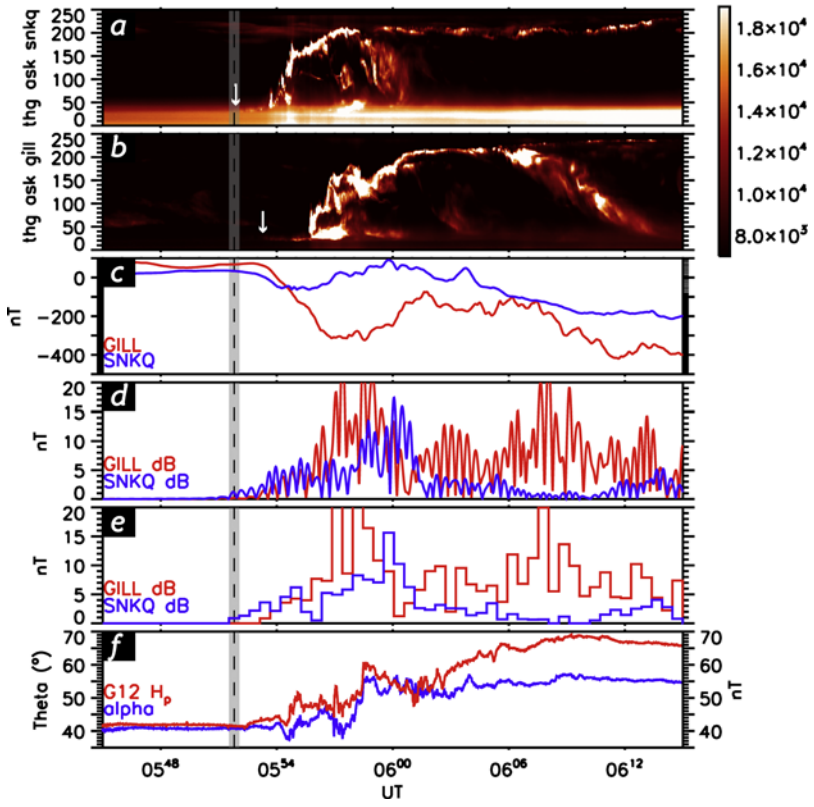

Figure 3. Substorm onset: 7 March 2007. North–south cuts (keograms) through the ASI FOV along a magnetic meridian from horizon to horizon at (a) SNKQ (at corrected geomagnetic (CGM) latitude 66.9°, longitude 356.4°, L = 6.50) and (b) GILL (CGM latitude 66.0°, longitude 332.8°, L = 6.04); color scale represents white light intensity. H component (magnetic N–S) (c) raw, (d) filtered transverse amplitude, and (e) power in the 24–96 s period band) from SNKQ (blue) and GILL (red). (f) GOES 12 magnetic field parallel to the satellite spin axis (Hp in blue; approximately parallel to the Earth's magnetic dipole moment), and α (in red) the angle between Hp and He (which points to the Earth center). The dashed vertical black line and the shaded gray region represent the 24–96 s SNKQ AWESOME-determined magnetic onset time and associated error (see text).

0700 UT on 7 March 2007, denoted by the red and blue lines, respectively. The dashed vertical line represents the onset of 24–96 s ULF wave activity at the SNKQ station at 0551:48 UT. Subsequent to the ULF wave onset, a moderate substorm is observed, identified by the development of ground magnetic bays of up to 400 nT in both H and D components, the most notable of which is the large H component bay at GILL.

[8] Figures 3a–3f provide an optical and magnetic overview of this substorm expansion as characterized by 250 bin keograms (time series of north–south cuts through zenith) from the two ASIs shown in Figure 1b, by the magnetometers colocated at these sites, and by the geosynchronous GOES 12 satellite. The SNKQ keogram shows a small arc feature at 0552 UT (denoted by the white arrow) at around bin 30 (~63.8°CGM latitude), approximately 90 s before the poleward auroral expansion in the SNKQ central meridian keogram. The keogram for the GILL ASI shows a similar small arc formation (denoted by the white arrow) and subsequent poleward expansion, both of which are slightly delayed by around 2 min as compared to SNKQ. Data from the magnetometer arrays shown in Figure 2 indicate the formation of the substorm current wedge [*McPherron et al.*, 1973]. The amplitude and power of transverse magnetic perturbations in the 24–96 s wavelet band show the onset of impulsive ultralow frequency (ULF) wave signatures believed to represent Alfvén waves which propagate to establish the field-aligned currents (FACs) in the substorm current wedge (SCW). Figure 3f shows the GOES 12 parallel component magnetic field (Hp being approximately parallel to the Earth's spin axis) and the angle α between Hp and the earthward directed magnetic field component, He. The vertical dashed line shows the onset time of the first impulsive ground magnetic signatures at SNKQ as determined from the DWT analysis using a Meyer wavelet basis as outlined by *Murphy et al.* [2009]. For this event, the first ground-based magnetic disturbance occurred in the 24–96 s wavelet band determined by AWESOME (see *Murphy et al.* [2009] for details on the technique) at SNKQ and subsequently at the surrounding stations, the SNKQ onset time being 0551:48 UT ± 16 s. We also applied DWT timing to the Hp time series from GOES 12, indicating an onset of magnetic disturbances in space at 0552:04 UT ± 16 s. The most rapid depolarization at GOES 12 occurs at approximately 0557:24 UT as indicated by an increase in α.

[9] We applied this DWT analysis to the 25 magnetometer stations available in the Canadian sector and Figure 4

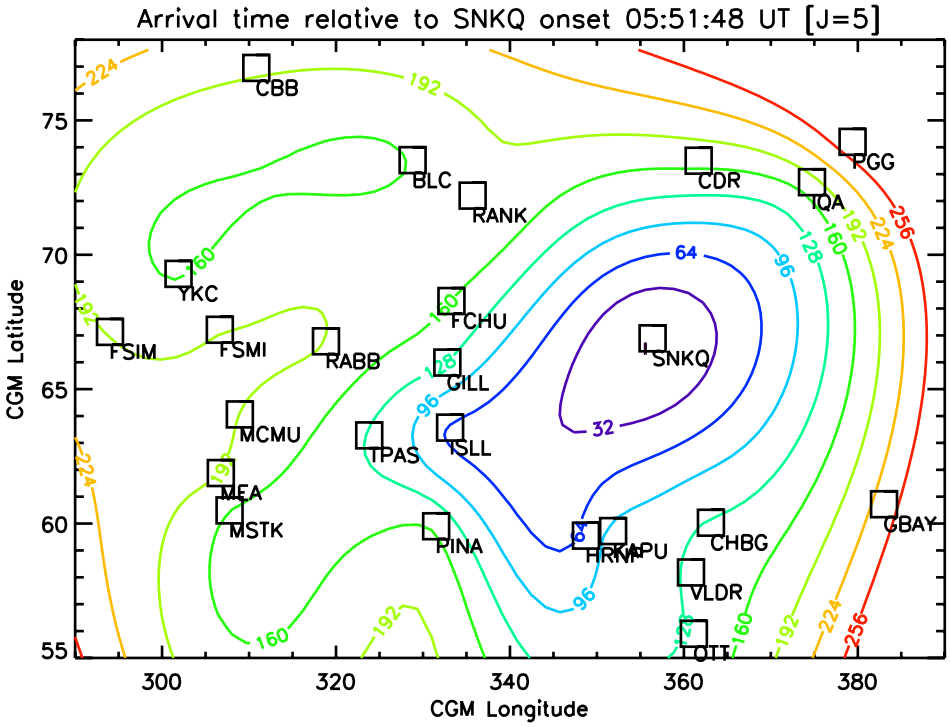

Figure 4. Magnetic substorm onset timing. A 2-D minimum curvature surface fit to the first magnetic disturbance (in the 24–96 s period wavelet band; see *Murphy et al.* [2009] for details) arrival time for 25 magnetometer stations across Canada as a function of CGM coordinates.

shows contours of the 24–96 s AWESOME-determined ground-based magnetic onset time relative to the SNKQ onset time at 0551:48 UT. There is a clear epicenter to the onset of the 24–96 s ULF waves on the ground, the delays showing a clear and coherent outward propagation away from a region close to the SNKQ station. *Milling et al.* [2008] found that the rate of expansion of the onset of Pi1 waves was approximately 1 MLT hour per 20 s in the east and west directions, which was consistent with the estimates of Pi2 expansion rates found by *Samson and Harrold* [1985], and much faster than the expansion of the auroral surge [cf. *Roux et al.*, 1991; *Angelopoulos et al.*, 2008]. In this case study, we find that the propagation direction is tilted with respect to lines of constant magnetic latitude, although detailed interpretation is limited by sparse longitudinal coverage. However, the first indication of Pi1 pulsation onset westward of the epicenter occurs ~2 MLT sectors away ~1 min later, reconfirming the result obtained by *Milling et al.* [2008].

[10] Figures 5a–5f show six pairs of images of ASI data from SNKQ and GILL that are false color (Figures 5a–5c) original images and (Figures 5d–5f) difference images between the current ASI images and the image from 3 s prior. We determined that the first optical onset occurred at 0551:54 UT (not shown) and Figure 5a at 0552:15 UT shows an example of the azimuthal, latitudinally confined arc undulations which develop along this faint arc at a magnetic latitude of 64° (L~5.5), approximately 3 degrees below the preexisting bright discrete aurora. The arc features are seen as bright spots with small azimuthal scale, in a localized region in the southwest of the SNKQ field of view (FOV) which can be clearly seen in both the original and differenced panels (see auxiliary material Animation S1 for the onset of ULF wave power and the formation and development of these auroral features). These arc undulations initially evolve at small azimuthal scales of ~70 km and show eastward phase propagation. The arc ripples merge into larger azimuthal scale features, before finally developing into a series of larger-scale (~100 km) vortical structures (see auxiliary material for details).[1] The vortices appear to develop a nonlinear and wrapped character before they eventually propagate poleward to the location of the most equatorward preexisting discrete arc [*Voronkov et al.*, 2000; *Lyons et al.*, 2002]. These preexisting arcs remain quasi-static on a 3 s time scale except for slow fading. Following this, at approximately 0554:30 UT, the structured arc system expands poleward and eventually develops into the WTS which is released from the region of the preexisting discrete arcs. In the GILL ASI FOV a similar merging of small-scale azimuthal features into larger-scale undulations occurs slightly later and ahead of the WTS. Interestingly, the small-scale features ahead of the WTS have a complicated phase structure which propagates both eastward and westward along a line of approximately constant geomagnetic latitude. Similar dynamics in an azimuthally extended auroral display have been described before in relation to a pseudobreakup [*Donovan et al.*, 2007] and pseudobreakups and substorm onsets [*Liang et al.*, 2008] though without the compelling ground-based and in situ magnetic observations presented here that clearly define onset. Comparing the keograms at SNKQ and GILL in Figure 3 with the ASI images in Figure 5 emphasizes the care required for accurate

[1] Auxiliary materials are available in the HTML. doi:10.1029/2008JA013771.

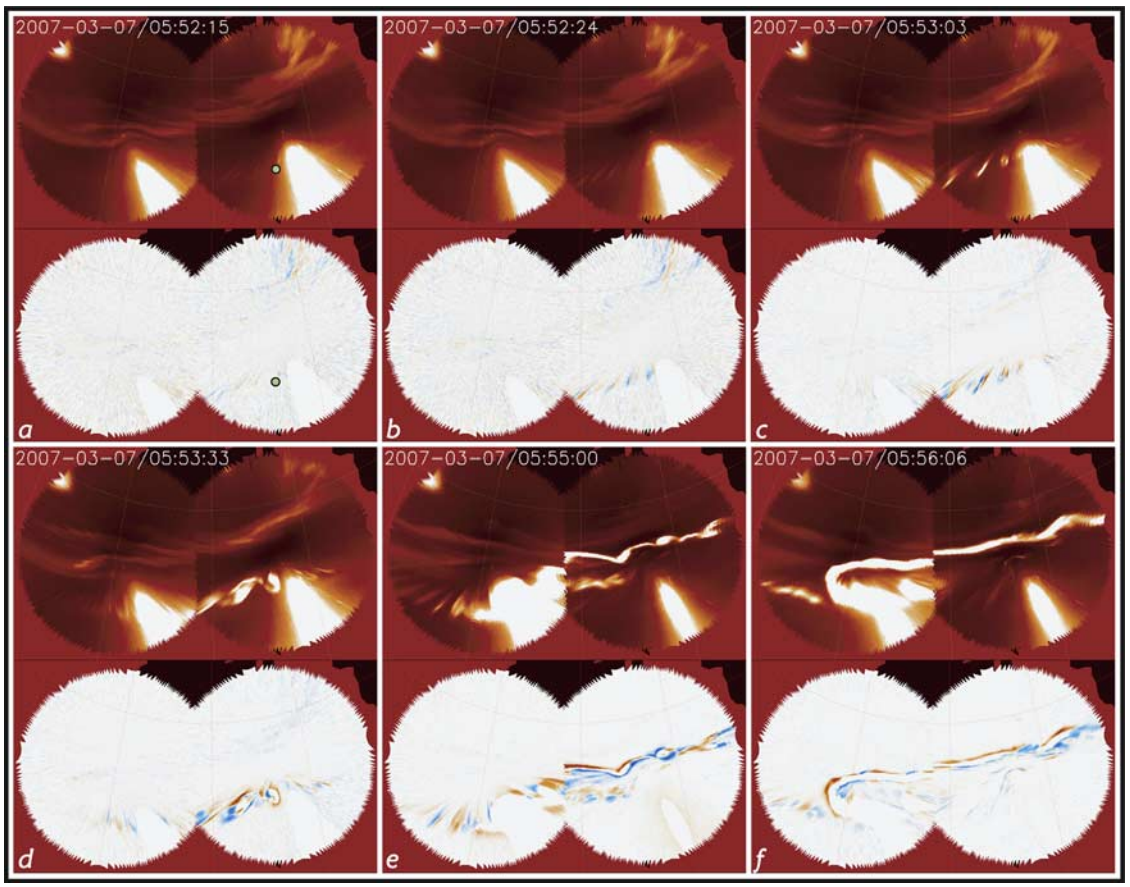

Figure 5. Substorm onset arc dynamics. ASI data from SNKQ and GILL from 0552:15 to 0556:06 UT, spanning the substorm onset. Time runs from left to right and top to bottom, and the emissions are overlaid on a geographic map. In each panel the top image shows a false color image of white light intensity, while the bottom image is a false color representation of the difference between the current ASI images and the image from 3 s prior. The bright region in the bottom right of each upper image shows the signature of the moon (not removed to maintain the integrity of the image). In the bottom images, red represents the appearance of new emissions, and blue represents the disappearance of prior emissions; the lunar signature is therefore removed. For context, the green and black dot in Figure 5a in the SNKQ FOV shows the T96 [*Tsyganenko*, 1995] tracing of the ground magnetic footprint of GOES 12.

optical timing of substorm onset on the ground especially when using meridian scanning instrumentation. The white arrows in Figure 3 indicate that the intensification and structuring of the equatorward onset arc evolve for around 2.5 min in advance of the auroral breakup which traditionally signifies substorm expansion phase onset. Observations from the cutoff of 486 nm emissions from the GILL NORSTAR meridian scanning photometer (not shown) indicate that the new arc system at GILL lies in the transition region between taillike and dipole-like field line topologies that is postulated to correspond to a region close to the inner edge of the ion plasma sheet [e.g., *Samson et al.*, 1992; *Friedrich et al.*, 2001] and a region that may be susceptible to, for example, the growth of the ballooning mode [e.g., *Roux et al.*, 1991; *Miura*, 2001] and the cross-field current instability [e.g., *Lui et al.*, 1991]. This indicates that the onset location, identified in the ionosphere by the onset of both optical arc disturbances and magnetic perturbations, is magnetically conjugate to the region expected to be unstable to the plasma instabilities [*Roux et al.*, 1991, *Lui et al.*, 1991; *Voronkov et al.*, 2000] hypothesized to instigate the substorm in the "inside-to-out" paradigm [*Samson et al.*, 1992; *Friedrich et al.*, 2001]. The evolution of 70 km arc ripples into 100 km vortices at onset seen here has been previously reported [*Friedrich et al.*, 2001] at ~1 min resolution, however, the cadence of our optical observations shows in detail at 3 s temporal resolution how this occurs via an inverse spatial cascade. The combination of the optical and magnetic onset signatures shown here demonstrate that not only are there no auroral disturbances in the preexisting poleward discrete arc region, but also that this region remains magnetically quiet, in advance of the development of the WTS.

[11] More importantly, the DWT magnetic timing identifies the ionospheric onset initiation region as SNKQ at the same time as the new optical auroral signature appears in the SNKQ ASI FOV within expected error. Although ground magnetometers Biot-Savart integrate the magnetic signatures from currents in the overhead ionosphere (on scales ~100 km), our results validate the utility of magnetic measurements for timing and locating the ionospheric substorm expansion phase onset epicenter with an accuracy of

~10 s even in cloudy conditions. Locating the SCW elements using the magnetic bays [*Cramoysan et al.*, 1995] across the combined magnetometer arrays shown in Figure 4 places the meridian of the downward FAC between KAPU and VLDR in the same meridian as SNKQ, the upward FAC element between TPAS and ISLL, and the electrojet latitude between GILL and ISLL (relevant station locations are also shown on Figure 4). The location of the subsequent downward FAC therefore appears to be coincident with the magnetic and optical onset location at SNKQ, suggesting that the location of the downward FAC and the onset initiation process may be intimately linked [*Milling et al.*, 2008].

[12] Finally, we note that the dipolar magnetic field strength at geosynchronous orbit is ~100 nT. In this interval, the magnetic field strength observed at GOES 12 is ~75 nT, which infers only a moderately stretched tail magnetic field configuration in the near-Earth region.

4. Discussion and Conclusions

[13] Our observations show that ionospheric substorm onset is characterized by a Pi1 magnetic disturbance whose onset propagates coherently away from a localized region. This has previously been impossible to achieve with Pi2 wave analyses [*Yumoto et al.*, 1990] since the more global and longer-period Pi2 disturbance occur coincidentally within one wave cycle across continental scales and onset is difficult to confidently identify at all stations. The smaller-period Pi1 magnetic onset time on the other hand is delayed with a coherent pattern of lag away from a localized epicenter. This epicenter is colocated with the region where spatially localized, latitudinally narrow small-scale (~70 km) undulations develop on a faint isolated arc which is located ~3° equatorward of the preexisting discrete auroral arcs. The pre-onset poleward discrete arc system remains spatially and temporally distinct from, and quasi-stable and unaffected by, the rapid dynamics of the new more equatorward auroral activity described in this paper during the first the 2–3 min following onset.

[14] In addition to revealing the combined characteristics of the new expansion phase onset arcs and Pi1 activity, the fact that the poleward arcs within the auroral oval remain undisturbed for such a long period while the more equatorward arcs develop on second time scales is also one of the most important elements of the results reported here. As reported by *Elphinstone et al.* [1995], during the expansion phase the auroral oval often exhibits a "double-oval" morphology, with activations at the poleward branch of this double oval occurring largely independent of activations on the lower-latitude branch. More generally, activations of the poleward boundary (termed poleward boundary intensifications (PBIs) [e.g., *Lyons et al.*, 1999]) occur relatively independent from the rest of the oval. Significantly, PBIs are often observed in association with Earthward flow bursts [*Lyons et al.*, 1999; *Zesta et al.*, 2000, 2002], especially in the case of those PBIs with a north-south (N–S) structure (known as auroral streamers [e.g., *Henderson et al.*, 1998]). Auroral streamers are often seen to propagate equatorward from the poleward border as expected for the ionospheric signature of inward propagating flows [*Zesta et al.*, 2000, 2002]. In the event reported here, the onset arc features and Pi1 waves evolved for around 2.5 min before the development of the auroral surge. Close to the onset location, there was no evidence for the development of auroral streamers traveling equatorward as might be expected if the onset Pi1 and auroral arc signatures developed as a result of, for example, the breaking of inward propagating flows across the plasma sheet. The absence of such signatures in the ionosphere represents a very serious challenge to the NENL hypothesis, since we assert that such flows may likely produce an auroral signature similar in morphology to a N-S auroral streamer. However, no such auroral form is seen in this event.

[15] We propose that the optical and magnetic manifestations of expansion phase onset initiation reported in this paper represent the ionospheric signature of a near-Earth plasma sheet instability [*Roux et al.*, 1991; *Lui et al.*, 1991; *Voronkov et al.*, 2000]. Such an instability might initiate substorm expansion phase onset in the magnetosphere via the "inside-to-out" model (A→B→C in Figure 1c), perhaps via a current disruption mechanism. Interestingly, Figure 3f also clearly shows evidence for a magnetic field rotation at geosynchronous orbit within ~20 s of the ground onset signatures which indicates onset activity at geosynchronous orbit ~2.5 min before auroral breakup. The ~20 s timing between geosynchronous and ground ULF onset is consistent with an Alfvén wave traveling along a dipolar field line, assuming a 1/cc number density and a ~100 nT magnetic field strength defines the slowest Alfvén speed. Note that it is not possible to resolve onset to better than half the wave period, either on the ground or in space; in this case, the associated errors are ±16 s. The ULF wave onset on the ground and in space could be as short as ~seconds apart or as long as ~30 s; shorter delay times between the magnetosphere and the ionosphere could be due to energetic electrons which have been accelerated via Shear Alfvén waves in the equatorial plane.

[16] As mentioned above, the competing NENL model [*Hones*, 1976; *Nagai et al.*, 1998] suggests flows released by NENL reconnection at ~20–30 R_E traverse the CPS and create onset arc development by processes such as flow braking [*Shiokawa et al.*, 1998] (C→A→B in Figure 1c). To explain our observations, any NENL model must explain why the higher-latitude ionosphere, which maps to the CPS, remains both optically and magnetically undisturbed for a period of ~2.5 min while the new onset related auroral arc rapidly evolves at L~5.5. To be consistent with NENL model, such behavior would require either an extreme stretching of the nightside magnetic field so that dipolar field lines must extend deep into the magnetotail, or the magnetosphere and ionosphere must be strongly decoupled. To address the former case, only geosynchronous in situ observations are available during this interval and the field configuration around geosynchronous seems to be only moderately stretched (a 1/3 reduction in local field strength at GEO). *Ge and Russell* [2006] showed that the field strength could approach ~5 nT during disturbed events around 8–9 R_E in the magnetotail two hours either side of midnight. Therefore, for magnetic connectivity between a hypothesized NENL and field lines that map to the auroral ionosphere, the field strength must drop quickly and significantly immediately outside geosynchronous orbits. In the alternate case, the magnetosphere and ionosphere must be

strongly decoupled, such that the Earthward flows which cross the CPS, must be essentially invisible in the ionosphere with no magnetic or auroral signature. Furthermore, such a NENL model must also explain why the onset of magnetic long-period Pi1 activity propagates coherently outward from a longitudinally localized onset in the ionosphere at L~5.5, despite a prior inward (equatorward) propagation of flow and information from the NENL through the CPS. Alternatively, if substorm onset is triggered by an ''inside-to-out'' process, auroral breakup could naturally be associated with reconnection at the NENL. Once outward propagating disturbances reached the NENL [*Friedrich et al.*, 2001], reconnection would subsequently cause auroral breakup explaining the 2.5 min delay. Regardless, our observations provide a remarkably tight constraint on the mechanisms responsible for the initiation of substorm onset (Figure 1c).

[17] Very recently, the THEMIS satellite constellation observed a causal sequence of energy release from magnetic reconnection at the NENL at a distance of ~20 R_E from the Earth, subsequent nearer Earth flows in the plasma sheet, and later still auroral brightenings and magnetic Pi2s attributed to energization by the NENL reconnection [*Angelopoulos et al.*, 2008]. The study of Angelopoulos *et al.* clearly demonstrated a causal ionospheric and auroral brightening response to NENL reconnection. However, in that case, the dominant ionospheric current response occurred at much higher latitudes than the substorm reported here, close to the poleward border, the largest magnetic response being confined to RANK latitudes with auroral zone stations only seeing evidence of smaller amplitude (tens of nT) current signatures. The difference in the observed ionospheric response between events such as that reported by *Angelopoulos et al.* [2008] and those similar to the substorm reported here may provide the clearest indication to as to the nature of the physical mechanisms responsible for the energy release in each case. Indeed, the substorm event we report here has an ionospheric morphology significantly different from that reported by *Angelopoulos et al.* [2008] suggesting that the processes operating were likely not the same.

[18] Uncertainty in mapping the ionospheric onset location to a specific distance down the equatorial magnetotail of course remains. However, the localized magnetic Pi1 signals and onset aurora, the contemporaneous signatures at geosynchronous orbit, and the lack of both magnetic and optical disturbances in the ionosphere at latitudes above L~5.5, suggest that these disturbances during the first seconds of onset map close to the Earth. Further conjugate multipoint satellite observations from the NASA THEMIS mission in the near-Earth plasma sheet should be able to finally determine the cause of the new lower-latitude magnetic and optical ionospheric substorm onset features we report here, validate their role in triggering substorm expansion phase onset, and establish whether such auroral substorm expansion phase onsets are explained by the ''inside-to-out model.''

[19] **Acknowledgments.** CARISMA is operated by the University of Alberta, funded by the CSA. I.R.M. was supported by an NSERC Discovery Grant. THEMIS was funded by NASA contract NAS5-02099. The authors thank NRCan for the provision of data from the Canadian Magnetic Observatory System (CANMOS) Network. Deployment of THEMIS GBOs in Canada was supported by a CSA contract to the University of Calgary. The NORSTAR MSPs are operated by the University of Calgary with funding from the CSA Canadian GeoSpace Monitoring program.

[20] Wolfgang Baumjohann thanks Gerhard Haerendel and another reviewer for their assistance in evaluating this paper.

References

Akasofu, S.-I. (1964), The development of the auroral substorm, *Planet. Space Sci.*, *12*, 273–282, doi:10.1016/0032-0633(64)90151-5.

Akasofu, S.-I., D. S. Kimball, and C.-I. Meng (1965), Dynamics of the aurora, II, Westward traveling surges, *J. Atmos. Terr. Phys.*, *27*, 173–174.

Angelopoulos, V., et al. (2008), Tail reconnection triggering substorm onset, *Science*, *321*, 931–935, doi:10.1126/science.1160495.

Baker, D. N., T. A. Fritz, R. L. McPherron, D. H. Fairfield, Y. Kamide, and W. Baumjohann (1985), Magnetotail energy storage and release during the CDAW 6 substorm analysis intervals, *J. Geophys. Res.*, *90*(A2), 1205–1216, doi:10.1029/JA090iA02p01205.

Cramoysan, M., R. Bunting, and D. Orr (1995), The use of a model current wedge in the determination of the position of substorm current systems, *Ann. Geophys.*, *13*, 583–594, doi:10.1007/s00585-995-0583-0.

Donovan, E. F., S. Mende, B. Jackel, M. Syrjasuo, M. Meurant, I. Voronkov, H. U. Frey, V. Angelopoulos, and M. Connors (2007), The azimuthal evolution of the substorm expansive phase onset, in *Proceedings of the Eighth International Conference on Substorms*, edited by M. Syrjäsuo and E. Donovan, pp. 55–60, Univ. of Calgary, Calgary, Alberta, Canada.

Elphinstone, R. D., et al. (1995), The double oval UV auroral distribution: 1. Implications for the mapping of auroral arcs, *J. Geophys. Res.*, *100*(A7), 12,075–12,092, doi:10.1029/95JA00326.

Friedrich, E., J. C. Samson, and I. Voronkov (2001), Ground-based observations and plasma instabilities in auroral substorms, *Phys. Plasmas*, *8*, 1104, doi:10.1063/1.1355678.

Ge, Y. S., and C. T. Russell (2006), Polar survey of magnetic field in near tail: Reconnection rare inside 9 R_E, *Geophys. Res. Lett.*, *33*, L02101, doi:10.1029/2005GL024574.

Henderson, M. G., G. D. Reeves, and J. S. Murphree (1998), Are north–south structures an ionospheric manifestation of bursty bulk flows?, *Geophys. Res. Lett.*, *25*, 3737–3740, doi:10.1029/98GL02692.

Hones, E. W., Jr. (1976), The magnetotail: Its generation and dissipation, in *Physics of Solar Planetary Environments: Proceedings of the International Symposium on Solar-Terrestrial Physics*, vol. 2, edited by D. J. Williams, pp. 558–571, AGU, Washington, D. C.

Jacobs, J., Y. Kato, S. Matsushita, and V. Troitskaya (1964), Classification of geomagnetic micropulsations, *J. Geophys. Res.*, *69*(1), 180–181, doi:10.1029/JZ069i001p00180.

Liang, J., E. F. Donovan, W. W. Liu, B. Jackel, M. Syrjäsuo, S. B. Mende, H. U. Frey, V. Angelopoulos, and M. Connors (2008), Intensification of preexisting auroral arc at substorm expansion phase onset: Wave-like disruption during the first tens of seconds, *Geophys. Res. Lett.*, *35*, L17S19, doi:10.1029/2008GL033666.

Lui, A. T. Y. (1991), A synthesis of magnetospheric substorm models, *J. Geophys. Res.*, *96*(A2), 1849–1856, doi:10.1029/90JA02430.

Lui, A. T. Y., C.-L. Chang, A. Mankofsky, H.-K. Wong, and D. Winske (1991), A cross-field current instability for substorm expansions, *J. Geophys. Res.*, *96*(A7), 11,389–11,401, doi:10.1029/91JA00892.

Lyons, L. R., T. Nagai, G. T. Blanchard, J. C. Samson, T. Yamamoto, T. Mukai, A. Nishida, and S. Kokubun (1999), Association between GEOTAIL plasma flows and auroral poleward boundary intensifications observed by CANOPUS photometers, *J. Geophys. Res.*, *104*, 4485–4500, doi:10.1029/1998JA900140.

Lyons, L. R., I. O. Voronkov, E. F. Donovan, and E. Zesta (2002), Relation of substorm breakup arc to other growth-phase auroral arcs, *J. Geophys. Res.*, *107*(A11), 1390, doi:10.1029/2002JA009317.

Mann, I. R., et al. (2008), The upgraded CARISMA magnetometer array in the THEMIS era, *Space Sci. Rev.*, *141*, 413–451, doi:10.1007/s11214-008-9457-6.

McPherron, R. L. (1972), Substorm related changes in the geomagnetic tail: The growth phase, *Planet. Space Sci.*, *20*, 1521–1539, doi:10.1016/0032-0633(72)90054-2.

McPherron, R. L. (1979), Magnetospheric substorms, *Rev. Geophys. Space Phys.*, *17*, 657–681, doi:10.1029/RG017i004p00657.

McPherron, R. L., C. T. Russell, and M. Aubry (1973), Satellite studies of magnetospheric substorms on August 15, 1978: 9. Phenomenological model for substorms, *J. Geophys. Res.*, *78*, 3131–3149, doi:10.1029/JA078i016p03131.

Mende, S. B., S. E. Harris, H. U. Frey, V. Angelopoulos, C. T. Russell, E. Donovan, B. Jackel, M. Greffen, and L. M. Peticolas (2008), The THEMIS array of ground based observatories for the study of auroral substorms, *Space Sci. Rev.*, *141*, 357–387, doi:10.1007/s11214-008-9380-x.

Milling, D. K., I. J. Rae, I. R. Mann, K. R. Murphy, A. Kale, C. T. Russell, V. Angelopoulos, and S. Mende (2008), Ionospheric localisation and expansion of long-period Pi1 pulsations at substorm onset, *Geophys. Res. Lett.*, *35*, L17S20, doi:10.1029/2008GL033672.

Miura, A. (2001), Ballooning instability as a mechanism of the near-Earth onset of substorms, *Space Sci. Rev.*, *95*, 387–398, doi:10.1023/A:1005249915285.

Murphy, K. R., I. J. Rae, I. R. Mann, D. K. Milling, C. E. J. Watt, L. Ozeke, H. U. Frey, V. Angelopoulos, and C. T. Russell (2009), Wavelet-based ULF wave diagnosis of substorm expansion phase onset, *J. Geophys. Res.*, *114*, A00C16, doi:10.1029/2008JA013548.

Nagai, T., M. Fujimoto, Y. Saito, S. Machida, T. Terasawa, R. Nakamura, T. Yamamoto, T. Mukai, A. Nishida, and S. Kokubun (1998), Structure and dynamics of magnetic reconnection for substorm onsets with Geotail observations, *J. Geophys. Res.*, *103*, 4419–4440, doi:10.1029/97JA02190.

Rae, I. J., et al. (2009), Timing and localization of ionospheric signatures associated with substorm expansion phase onset, *J. Geophys. Res.*, *114*, A00C09, doi:10.1029/2008JA013559.

Roux, A., S. Perraut, P. Robert, A. Morane, A. Pedersen, A. Korth, G. Kremser, B. Aparicio, D. Rodgers, and R. Pellinen (1991), Plasma sheet instability related to the westward traveling surge, *J. Geophys. Res.*, *96*(A10), 17,697–17,714, doi:10.1029/91JA01106.

Russell, C. T., et al. (2008), THEMIS ground-based magnetometers, *Space Sci. Rev.*, *141*, 389–412, doi:10.1007/s11214-008-9337-0.

Samson, J. C., and B. G. Harrold (1985), Characteristic time constants and velocities of high-latitude Pi 2's, *J. Geophys. Res.*, *90*(A12), 12,173–12,181.

Samson, J. C., L. R. Lyons, P. T. Newell, F. Creutzberg, and B. Xu (1992), Proton aurora and substorm intensifications, *Geophys. Res. Lett.*, *19*, 2167–2170, doi:10.1029/92GL02184.

Shiokawa, K., et al. (1998), High-speed ion flow, substorm current wedge, and multiple Pi 2 pulsations, *J. Geophys. Res.*, *103*, 4491–4507, doi:10.1029/97JA01680.

Sibeck, D. G., and V. Angelopoulos (2008), THEMIS science objectives and mission phases, *Space Sci. Rev.*, *141*, 35–59, doi:10.1007/s11214-008-9393-5.

Singer, H. J., L. Matheson, R. Grubb, A. Newman, and S. D. Bouwer (1996), Monitoring space weather with the GOES magnetometers, *Proc. SPIE Int. Soc. Opt. Eng.*, *2812*, 299–308.

Tsyganenko, N. A. (1995), Modeling the Earth's magnetospheric magnetic field confined within a realistic magnetopause, *J. Geophys. Res.*, *100*, 5599–5612, doi:10.1029/94JA03193.

Voronkov, I., R. Rankin, P. Frycz, V. T. Tikhonchuk, and J. C. Samson (1997), Coupling of shear flow and pressure gradient instabilities, *J. Geophys. Res.*, *102*(A5), 9639–9650, doi:10.1029/97JA00386.

Voronkov, I., E. F. Donovan, B. J. Jackel, and J. C. Samson (2000), Large-scale vortex dynamics in the evening and midnight auroral zone: Observations and simulations, *J. Geophys. Res.*, *105*(A8), 18,505–18,518, doi:10.1029/1999JA000442.

Yumoto, K., K. Takahashi, T. Sakurai, P. R. Sutcliffe, S. Kokubun, H. Lühr, T. Saito, M. Kuwashima, and N. Sato (1990), Multiple ground-based and satellite observations of global Pi 2 magnetic pulsations, *J. Geophys. Res.*, *95*(A9), 15,175–15,184, doi:10.1029/JA095iA09p15175.

Zesta, E., L. R. Lyons, and E. Donovan (2000), The auroral signature of Earthward flow burst observed in the Magnetotail, *Geophys. Res. Lett.*, *27*, 3241–3244, doi:10.1029/2000GL000027.

Zesta, E., E. Donovan, L. Lyons, G. Enno, J. S. Murphree, and L. Cogger (2002), Two-dimensional structure of auroral poleward boundary intensifications, *J. Geophys. Res.*, *107*(A11), 1350, doi:10.1029/2001JA000260.

V. Angelopoulos and C. T. Russell, Institute of Geophysics and Planetary Physics, University of California, Los Angeles, CA 90095-1567, USA.

E. F. Donovan, Department of Physics and Astronomy, University of Calgary, Calgary, AB T2N 1N4, Canada.

M. J. Engebretson, Department of Physics, Augsburg College, 2211 Riverside Avenue South, Minneapolis, MN 55454, USA.

H. U. Frey and S. B. Mende, Space Sciences Laboratory, University of California, 7 Gauss Way, Berkeley, CA 94720-7450, USA.

A. Kale, I. R. Mann, D. K. Milling, K. R. Murphy, I. J. Rae, G. Rostoker and C. E. J. Watt, Department of Physics, University of Alberta, Edmonton, AB T6G 2G7, Canada. (jrae@phys.ualberta.ca)

M. B. Moldwin, Department of Earth and Space Sciences, University of California, 595 Charles Young Drive East, Los Angeles, CA 90095-1567, USA.

H. J. Singer, NOAA Space Environment Center, 325 Broadway, Boulder, CO 80305, USA.